

# Numerical study of brash ice loads on ship hulls based on DEM-CFD

Tengchao Lu <sup>1</sup>; Zaojian Zou <sup>1,2</sup>

School of Naval Architecture, Ocean and Civil Engineering, Shanghai Jiao Tong University, Shanghai  
200240, China, 403979181@qq.com

2. Collaborative Innovation Center for Advanced Ship and Deep-Sea Exploration, Shanghai 200240,  
China

**Key words:** *Numerical simulation, Brash ice loads, Coupling DEM-CFD, Hertz-Mindlin (no-slip) contact model*

The brash ice loads on ship hulls are studied by coupling Discrete Element Method (DEM) and Computational Fluid Dynamics (CFD). The loads induced by brash ice on ship hulls and the interactions between ice floes are investigated by DEM. The hydrodynamics of ice floes, mainly including the drag force and the buoyance, is calculated by CFD. In the simulation, the ice floes are treated as discrete elements, and the ship hull is treated as rigid body with a certain speed. The contact forces between ice floes and ship hulls are determined by the Hertz-Mindlin (no-slip) contact model. The shape of ice floes is an approximate square composed of a number of spherical faces, which can reduce the computation cost. A validation of this method by comparison with the experiment data is presented. The numerical results show qualitative agreement with the experiment result. The reasons of deviations between numerical results and experiment data are discussed.

## 1. Introduction

With the acceleration of the global warming, the temperature of the Arctic has increased sharply. The abundant natural resources in the Arctic and the Arctic Passage that has economic importance and strategic value are taking the attention of the world. The exploration of the Arctic needs a large amount of ice-sailing ships. When designing ships adapted to the Arctic region, the investigation of ice loads on ship hulls plays a key role.

Normally, there exist four typical sea ice conditions: level ice, brash ice, ice ridge and iceberg. And ice-sailing ships usually follow sea path covered with brash ice broken by an icebreaker. Therefore, many researchers invested the brash ice load on ship hulls by several different methods, which include the experiments and numerical simulations. Because experiments are time consuming, expensive, and often limited by the available facility size and other physical constraints, and with the rapid development of numerical techniques and computation hardware, numerical simulation is becoming a very powerful tool to study the brash ice loads on ship hulls.

Because of the discrete characteristics of brash ice, the DEM has intrinsic advantages in simulations of ice-ship interactions. DEM was first proposed by Cundall in 1971 to simulate the behaviour of jointed rocks [1]. Since then, DEM has been applied to the problems of brash ice via independent codes and commercial software. In 1994, Sveinung Løset applied the soft particle approach to an ensemble of circular discs [2]. In the simulation, a boom was pulled through the ice floes, which are represented by 2D circular discs. The relationships between the ice load and boom width, ice concentration and drift speed were analysed [3]. In 1999, Hansen and Løset use the similar method to simulate the ice load on floating offshore unit moored in broken ice field on a set of different conditions, such as ice concentration and

towing velocities [4]. And the deviations between predicted and experiment results are explained [5]. In 2001, the 3D disk element was proposed by Hopkins to calculate the interaction between ice and wave, and between ice and offshore structures [6]. Zhan et al.(2010) and Lau et al. (2011) simulated the ice breaking and maneuvering abilities of an icebreaker with the DEM software named DECICE[7,8]. In 2013, Ji Shunying used DEM to simulate the interaction between drifting ice floes and a moving ship [9]. The ice floes are modelled by 3D dilated disks. In 2014, Li Baohui proposed a modified DEM for sea ice dynamics is developed based on the granular material rheology [10]. In 2016, Yulmetov simulated the progress of iceberg towing in broken ice with non-smooth DEM [11], and then validated the predicted result by comparing with experiment data [12].

With respect to the hydrodynamics on ice floes, there are different approaches to the problem. One method is to regard the hydrodynamics as the sum of water drag force and buoyancy. The drag force can be estimated by drag coefficient, which is related to the fluid properties and the shape of ice floe. This method ignores the influence of ice floes on water. Therefore, it is too simplistic to represent reality. Another way to invest the hydrodynamics is based on potential or viscous flow. In 2007, a numerical model based on Navier-Stokes solver was adopted by Gagnon to account for the fluid component[13]. In 2014, Andrei Tsarau et al. proposed a numerical model to analyse the hydrodynamic aspects of the interaction between a floating structure and surrounding ice based on potential flow[14]. However, these methods are computationally demanding and requires a supercomputer.

In this paper, the interaction between ice floes and a ship hull was simulated by coupling DEM and CFD. And the global ice resistance on the ship hull was obtained. The Hertz-Mindlin(no slip) contact model was adopted to calculate the contact force due to its accuracy and efficiency. In this model, the normal force component is based on Hertzian contact theory[15], and the tangential force component is based on Mindlin-Deresiewicz work[16, 17]. The hydrodynamics on ice floes are calculated by freestream equation based on drag coefficient. And the influence of ice floes on fluid is also taken into consideration. Two commercial software EDEM and Fluent are adopted to couple DEM and CFD. The data exchange is through a coupling interface. In addition, the results were discussed by comparing with the experiments results.

## 2. Numerical models

The simulation of the interaction between ice floes and ship hulls requires calculating several kinds of forces. These forces are mainly the contact force, gravity, buoyancy, and drag force.

### 2.1 Contact dynamics

The conventional DEM allows modelling deformable particles as well as complex shapes (from the ellipsoid to the polygon). The main assumptions of the contact dynamics (collision) model are: the particles are spherical and quasi-rigid, collisions are binary and instantaneous with a contact point, interaction forces are impulsive and all other finite forces are negligible during collision, motion is two-dimensional with the particle mass center moving in one plane, and both the restitution and the friction coefficients are constant in a simulation.

The motion of each individual ice floe is governed by the laws of linear momentum conservation (Newton's second law of motion) and angular momentum:

$$m_p \frac{d \vec{v}_p}{dt} = m_g \vec{g} + \vec{F}_{C,p} + \vec{F}_{D,p} + \vec{F}_{B,p} \quad (1)$$

$$I_p \frac{d\vec{\omega}_p}{dt} = \vec{T}_p \quad (2)$$

where  $m_p$ ,  $\vec{v}_p$  represent mass, velocity of the ( $p$  th) unit respectively;  $g$  is acceleration due to gravity;  $\vec{F}_{C,p}$  is the vector of contact forces (normal force and tangential force) between the particles;  $\vec{F}_{D,p}$  is the drag force,  $\vec{F}_{B,p}$  is the buoyancy force;  $I_p$  and  $\vec{\omega}_p$  are the moment of inertia and angular velocity;  $\vec{T}_p$  is the torque arising from the tangential components of the contact force.

According to the Hertz-Mindlin (no slip) contact model, the contact force  $\vec{F}_{C,p}$  can be divided in to two opponents. The normal force  $F_n$  is a function of normal overlap  $\delta_n$  and is given by

$$F_n = \frac{4}{3} E^* \sqrt{R^*} \delta_n^{\frac{3}{2}} \quad (3)$$

Where the equivalent Young's Modulus  $E^*$  and the equivalent radius  $R^*$  are defined as

$$\frac{1}{E^*} = \frac{1-\nu_i^2}{E_i} + \frac{1-\nu_j^2}{E_j} \quad (4)$$

$$\frac{1}{R^*} = \frac{1}{R_i} + \frac{1}{R_j} \quad (5)$$

Where  $E_i$ ,  $\nu_i$ ,  $R_i$  and  $E_j$ ,  $\nu_j$ ,  $R_j$  are the Young's Modulus, Poisson ratio and Radius of each sphere in contact.

The normal damping force  $F_n^d$  is given by

$$F_n^d = -2\sqrt{\frac{5}{6}}\beta\sqrt{S_n m^*} v_n^{rel} \quad (6)$$

Where  $v_n^{rel}$  is the normal component of the relative velocity,  $\beta$ ,  $S_n$ , and  $m^*$  are defined as

$$\beta = \frac{\ln e}{\sqrt{\ln^2 e + \pi^2}} \quad (7)$$

$$S_n = 2E^* \sqrt{R^* \delta_n} \quad (8)$$

$$\frac{1}{m^*} = \frac{1}{m_i} + \frac{1}{m_j} \quad (9)$$

Where  $e$  is the coefficient of restitution.

The tangential force  $F_t$  depends on the tangential overlap  $\delta_t$  and the tangential stiffness  $S_t$ .

$$F_t = -S_t \delta_t \quad (10)$$

$$S_t = 8G^* \sqrt{R^* \delta_n} \quad (11)$$

Where  $G^*$  is the equivalent shear modulus. Tangential damping force is given by

$$F_t^d = -2\sqrt{\frac{5}{6}}\beta\sqrt{S_t m^*} v_t^{rel} \quad (12)$$

Where  $\vec{v}_i^{rel}$  is the relative tangential velocity. The tangential force is limited by Coulomb friction  $\mu F_n$  where  $\mu$  is the coefficient of static friction.

The rolling friction is accounted for by applying a torque to the contacting surfaces.

$$\tau_i = -\mu_r F_n R_i \omega_i \quad (13)$$

Where  $\mu_r$  is the coefficient of rolling friction,  $R_i$  is the distance of the contact point from the center of mass and  $\omega_i$  is the unit angular velocity vector of the object at the contact point.

## 2.2 CFD approach

In this work, the commercial software Fluent was adopted to solves the Reynolds-Averaged Navier–Stokes (RANS) equations for incompressible flow by employing a finite volume discretization approach . The turbulence model was chosen to use  $k - \varepsilon$  model, which largely applied for its simplicity.

## 2.3 Coupling DEM-CFD

For coupling DEM-CFD, The CFD is performed as a single phase, transient calculation which is iterated to convergence for a time step. A drag force is then calculated on the DEM particles using the fluid velocity in the mesh cell within which each particle is located. The DEM then takes control of the simulation and performs one or more iterations. After the DEM finishes iterating, control is passed back to the CFD. A momentum sink is added to each of the mesh cells to represent the effect of energy transfer to the DEM particles. The Lagrangian coupling scheme is shown in Fig.1.

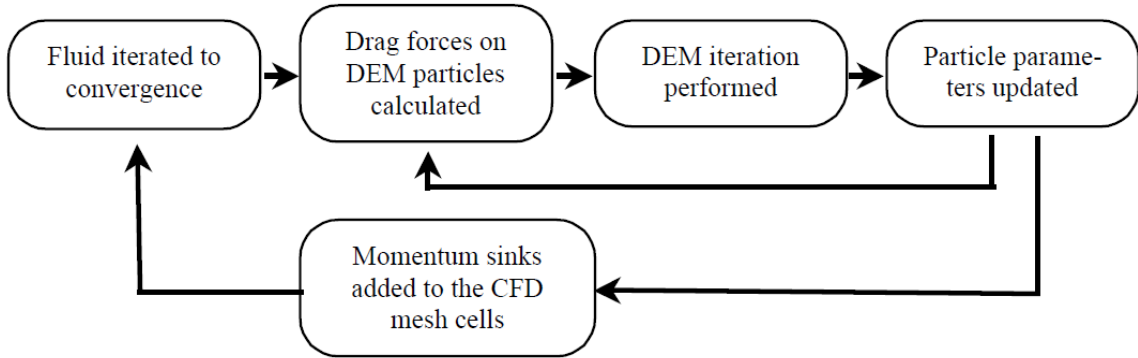


Fig.1 Schematic of Coupling Scheme

The momentum conservation equation can be written as

$$\frac{\partial \rho u}{\partial t} + \nabla \cdot \rho u u = -\nabla \rho + \nabla \cdot (\mu \nabla u) + \rho g - S \quad (14)$$

In Eq. (14),  $S$  is the magnitude of the momentum sink of the fluid mesh cell. The coupling of DEM and CFD can be implemented by calculating  $S$  with Eq. (15):

$$S = \frac{\sum_i^n F_i}{V} \quad (15)$$

Where  $F$  is the force on particle from the fluid,  $V$  is the volume of the fluid mesh cell.

The fluid drag force on each particle is calculated used a modified spherical, free-stream drag model. For non-spherical particles, the drag force is calculated based on a bounding

sphere. All fluid parameters are taken from the CFD mesh element which contains the centre of the DEM particle. The drag coefficient  $C_D$  depends on the Reynolds number  $Re$  :

$$Re = \frac{\alpha \rho L |v|}{\mu} \quad (16)$$

$$C_D = \begin{cases} \frac{Re}{24} & Re \leq 0.5 \\ 24(1.0 + 0.15 Re^{0.687}) / Re & 0.5 < Re \leq 1000 \\ 0.44 & Re > 1000 \end{cases} \quad (17)$$

where  $\rho$  is the fluid density,  $\mu$  is the fluid viscosity,  $L$  is the diameter of the particle's bounding sphere, and  $v$  is the relative velocity between the fluid and the particle.  $\alpha$  is the free volume of the CFD mesh cell.

The drag force is calculated by

$$F_d = 0.5 C_D \rho A |v| v \quad (18)$$

Where  $A$  is the projected area of the particle.

The buoyancy is calculated by

$$F_B = -\rho g V \quad (19)$$

### 3. Numerical simulation setup

In this paper, the numerical simulation setup is according to the experiment conducted by Løset in Hamburgische Schiffbau Versuchsanstalt GmbH (HSV) ice tank in 1998[18].

To reduce the calculation consumption, the dimensions of calculation domain are 30m long  $\times$  10m wide  $\times$  2.5m deep. The ship model is replaced by a simple polyhedron. Fig 1 shows the fluid domain geometric and mesh.

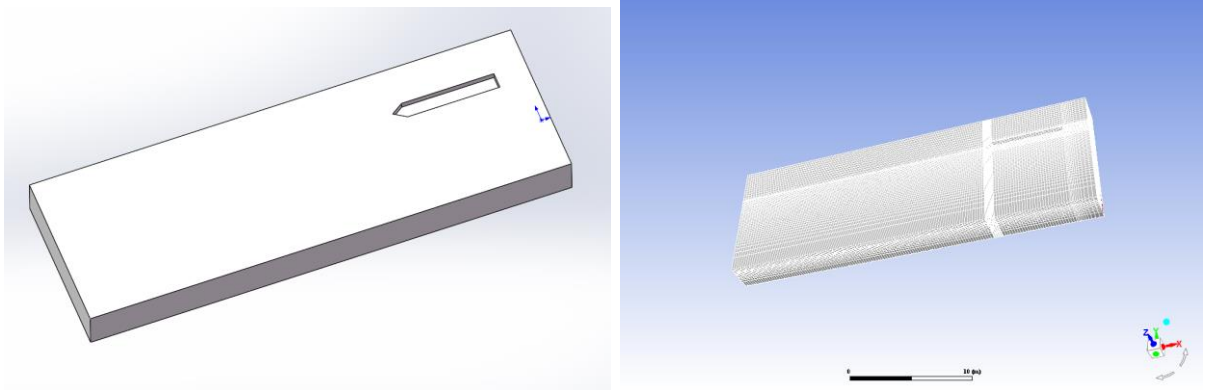


Fig.2 The fluid domain geometric and mesh

As shown in Fig3, a piece of ice floe is an approximate square made up by  $19 \times 19$  spheres. The sphere radius is equal to the thickness of ice floes. Therefore, the mass of the ice floes in simulation is smaller than those in the experiments. Other parameters of ice floes are shown in Table 1.

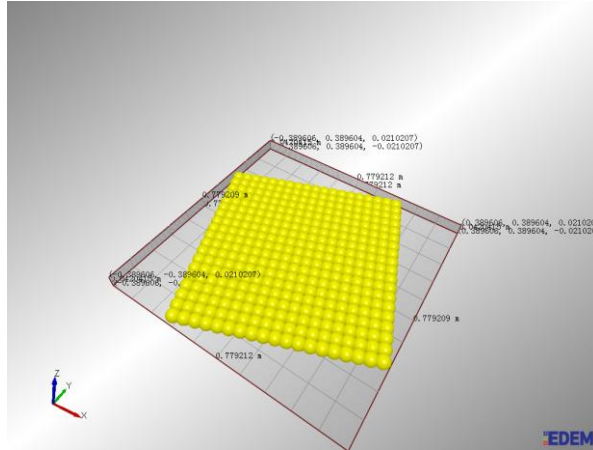


Fig.3 A piece of ice floe made up by spheres

Table 1. Parameters of ice floe

Parameter	Definition	Value
d	Thickness( $m$ )	0.042
L	Length of square ice floe( $m$ )	0.6
$\rho$	Density of ice( $kg / m^3$ )	900
E	Young's modulus ( $MPa$ )	40
$\nu$	Poisson's Ratio	0.3
$\mu$	Coefficient of static friction	0.4
e	Coefficient of restitution	0.2

By generating different quantities of ice floes in a certain area, the concentration of ice floes can be controlled. In this study, the concentration of ice floe is 90%. Fig. 4 shows the initial condition of the simulation in EDEM. In order to validate the predicted result by comparing with experiment data, three towing velocity, 0.05m/s, 0.75m/s and 0.125m/s are adopted.

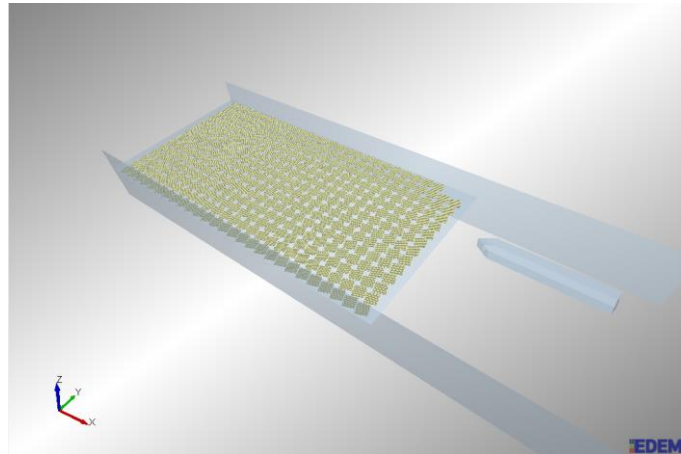


Fig.4 The initial condition of the simulation in EDEM

#### 4. Numerical simulation result

As shown in Fig. 5, in the simulation progress, the motion of ice floes in fluid caused by hydrodynamics and the interaction of between ice floes and the ship hull can be observed.

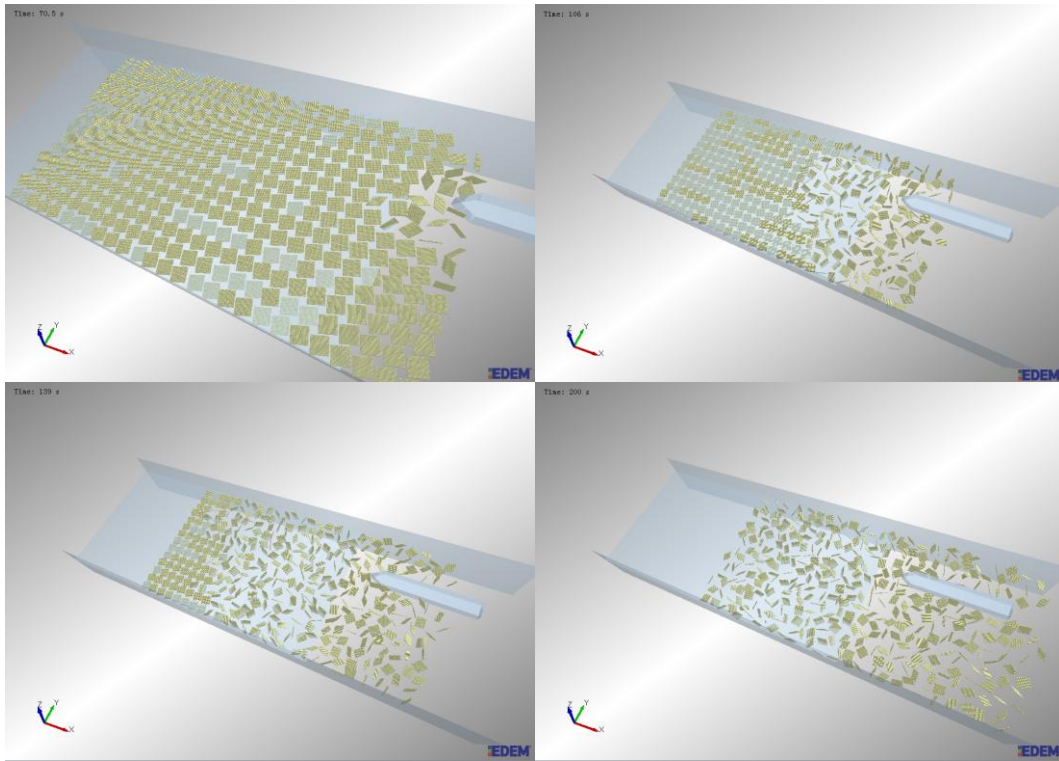


Fig.5 The simulation progress

Fig.6 shows the average velocity of ice floes in the simulation. At the start of simulation, the ice floes are static. And on the effect of drag force by the fluid, the ice floes began to move until reached the value of velocity of fluid.

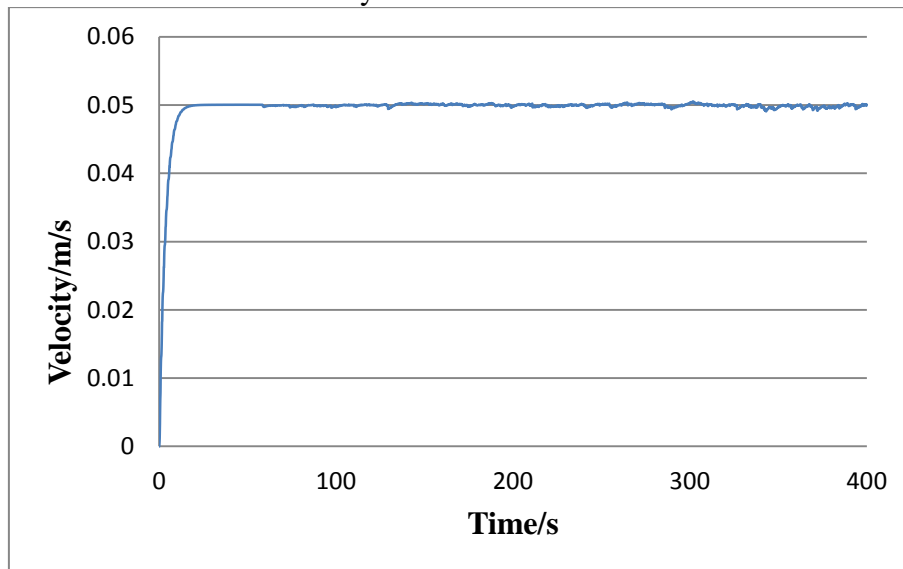
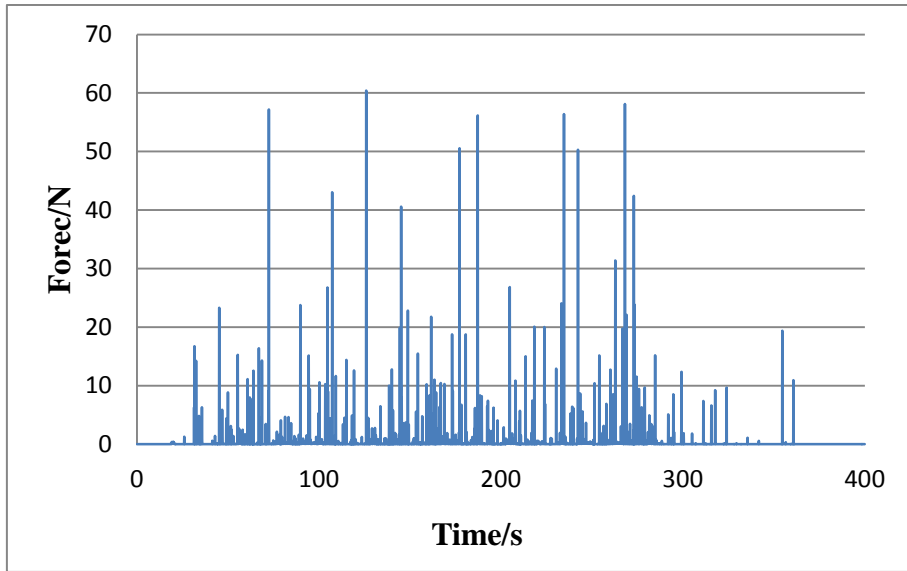
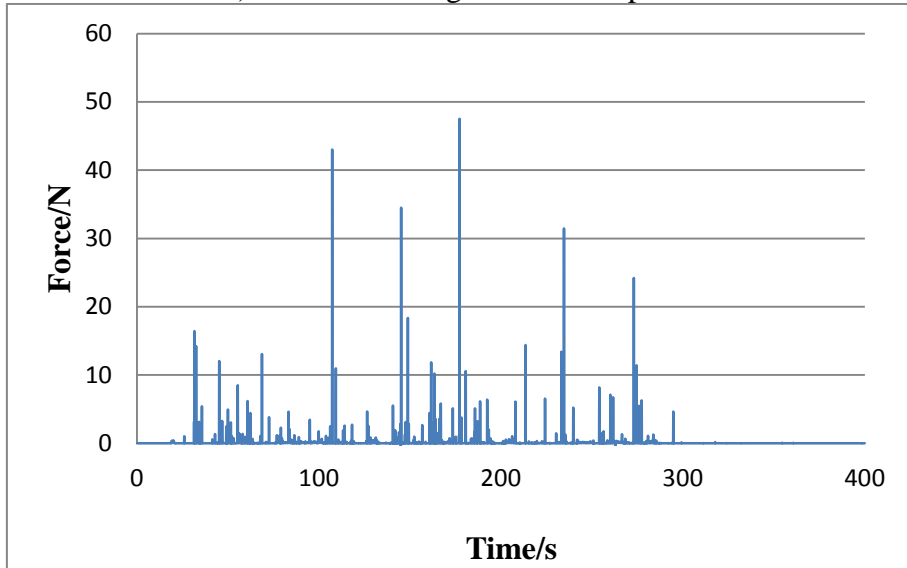


Fig.6 The average velocity of ice floes in simulation

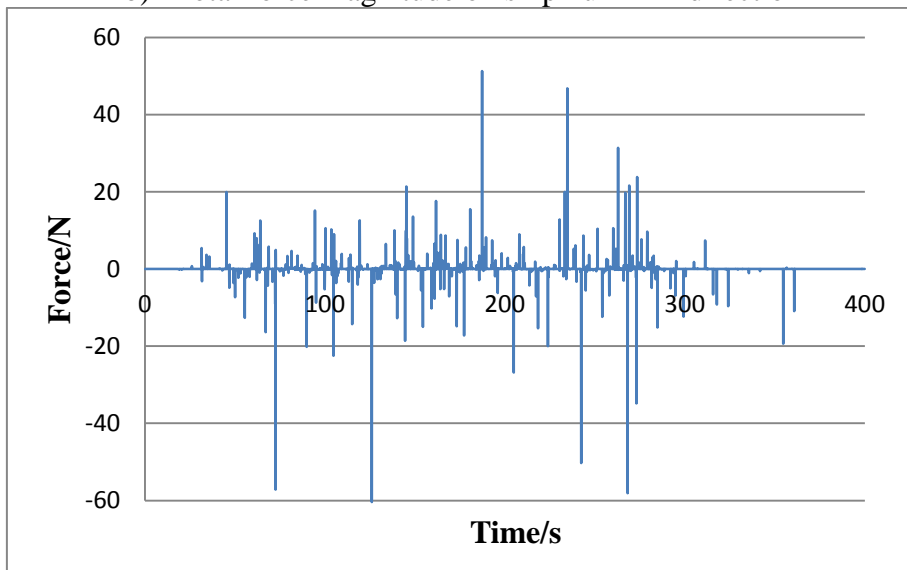
Fig.7, Fig.8 and Fig.9 shows the total force, total force in X direction and total force in Y direction on ship hull caused by the ice floes when the velocity equal to 0.05m/s, 0.075m/s and 0.0125m/s. As shown in the pictures, the the resistance curve is not continuous. Because during the time ship hull collides with a piece of ice floe, the contact force is much larger than the time without collision. And the time step of DEM is very small. In order to save storage space, the interval of data saving is relatively large. Therefore, the loss of data is inevitable.



a) Total fore magnitude on ship hull

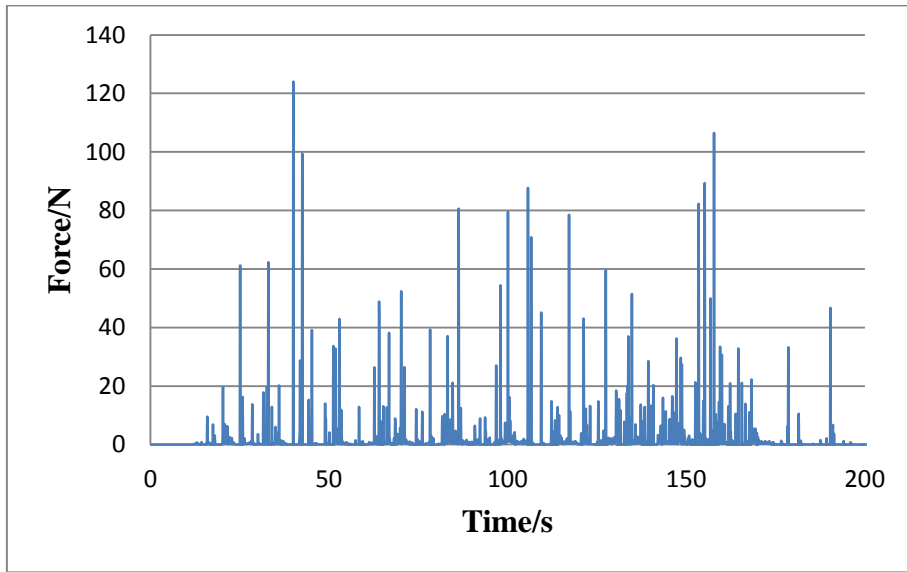


b) Total force magnitude on ship hull in X direction

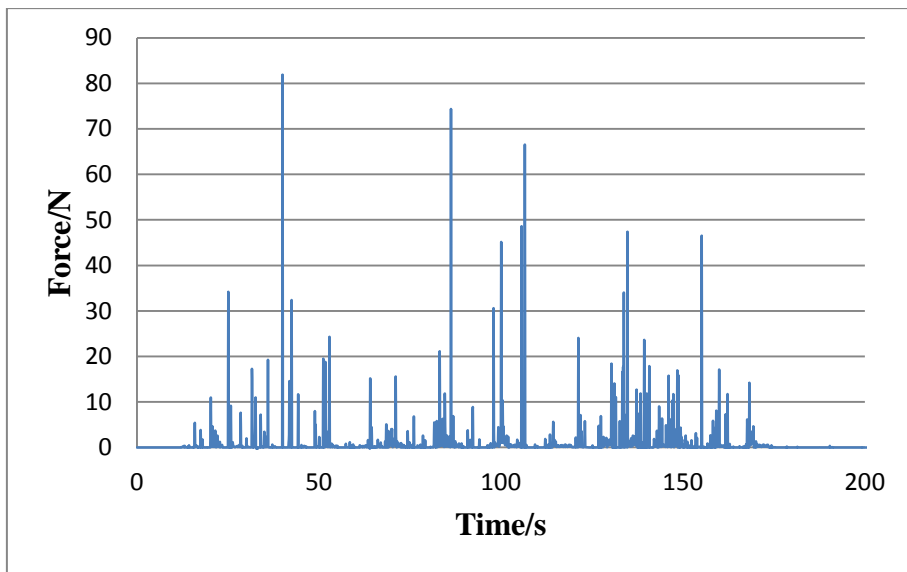


c) Total force magnitude on ship hull in Y direction

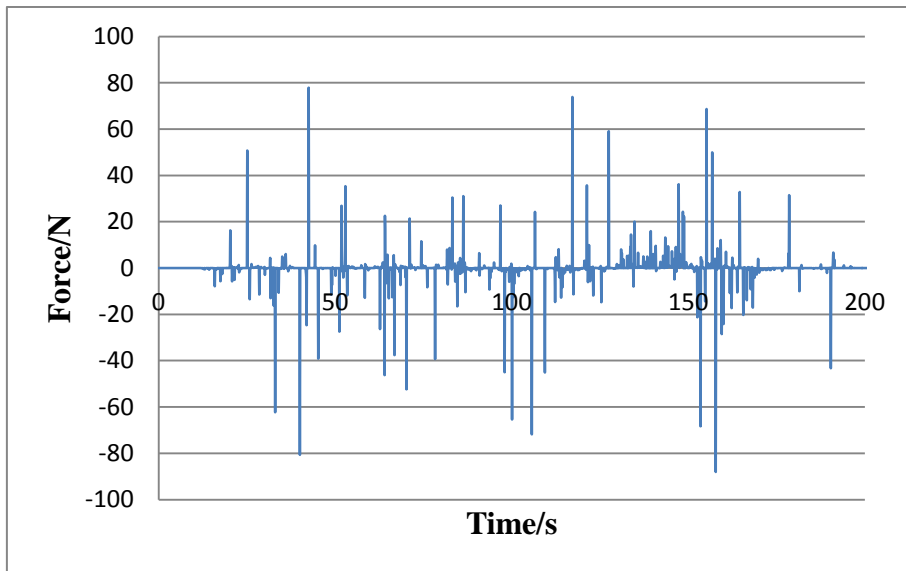
Fig.7 Velocity equal to 0.05m/s, the ice resistance on ship hull



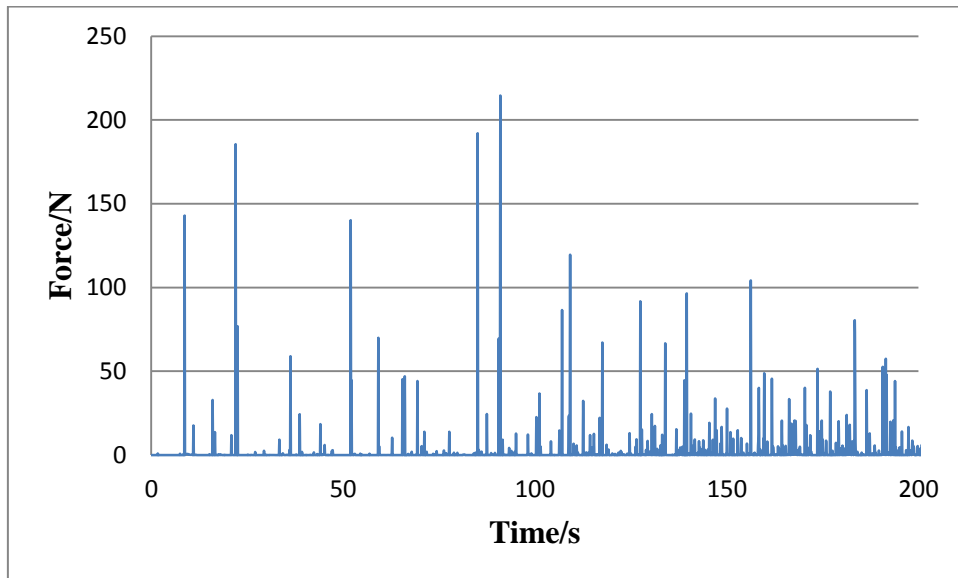
a) Total fore magnitude on ship hull



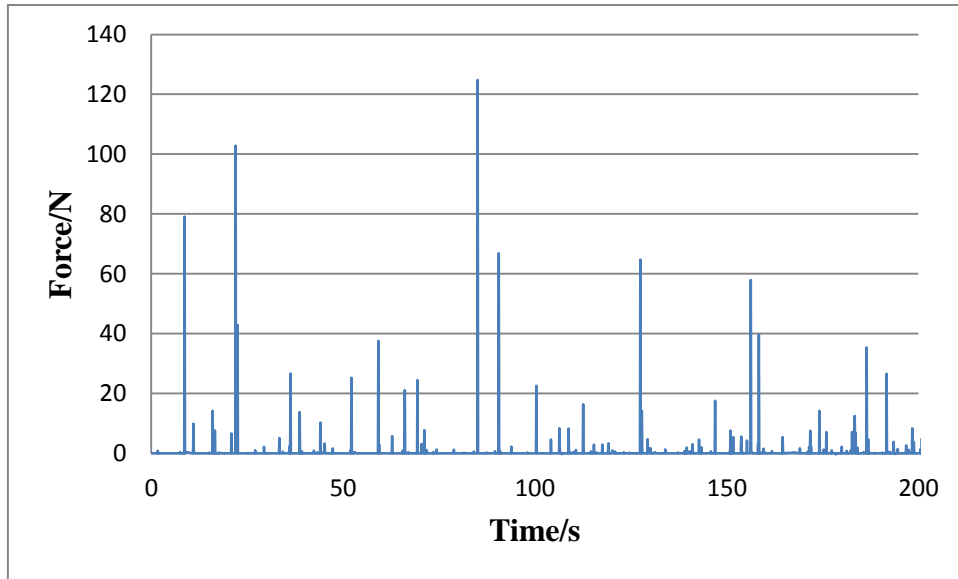
b) Total force magnitude on ship hull in X direction



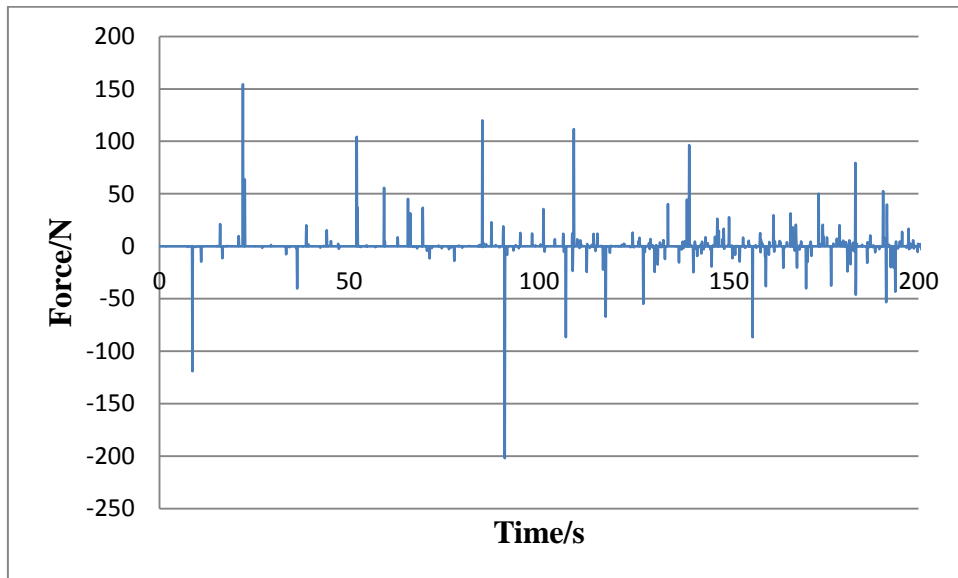
c) Total force magnitude on ship hull in Y direction  
Fig.8 Velocity equal to 0.075m/s, the ice resistance on ship hull



a) Total fore magnitude on ship hull



b) Total force magnitude on ship hull in X direction



c) Total force magnitude on ship hull in Y direction

Fig.9 Velocity equal to 0.125m/s, the ice resistance on ship hull

Fig.10 shows the comparison between simulation and experiment result. As the picture shows, the resistance of ice increases with the increase of velocity. By adjusting the simulation parameters, the simulation result could be in good agreement with the experiment result to a certain extent.

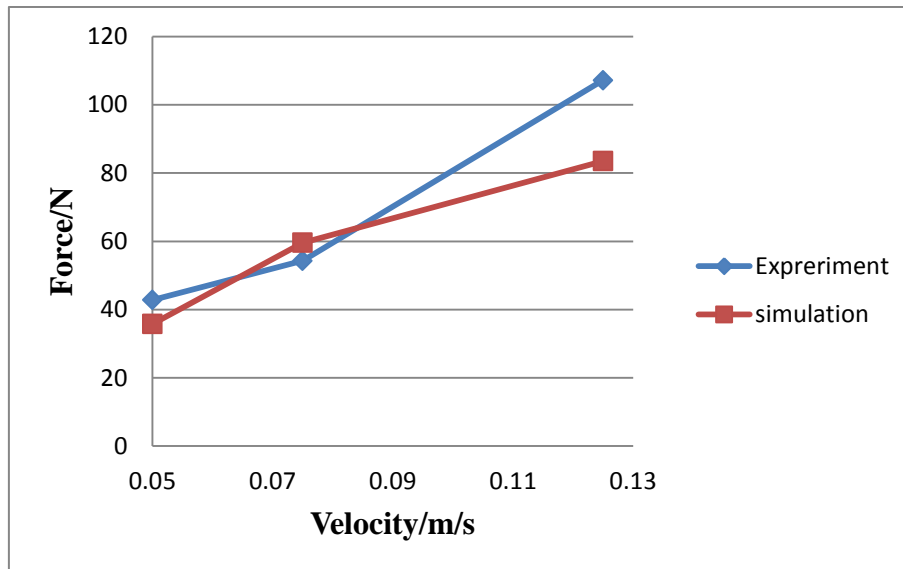


Fig.10 Comparison between simulation and experiment result

## 5. Conclusions

A numerical method to simulate the interaction between brash ice and ship hulls is introduced in this paper. By coupling DEM and CFD, the effect of the ice motion on fluid is taken in to consideration. The ice floes are approximate squares made up by spheres. This treatment can meet two requires: making the ice floes close to reality and reducing computation time. Therefore, the simulation can present the translation and rotation of ice floes. And the result obtained was validated by comparing experiment data.

## References

- [1] Cundall PA. A computer model for simulating progressive, large scale movements in blocky rock systems. Paper no. II-8.Proceedings of the Symposium of the International Society for RockMechanics; 1971 Oct; Nancy (France): International Society for Rock Mechanics.
- [2] Løset S. Discrete element modelling of a broken ice field — Part I: model development[J]. Cold Regions Science & Technology, 1994, 22(4):339-347.
- [3] Løset S. Discrete element modelling of a broken ice field — Part II: simulation of ice loads on a boom [J]. Cold Regions Science & Technology, 1994, 22(4):339-347.
- [4] Hansen E H, Løset S. Modelling floating offshore units moored in broken ice: model description [J]. Cold Regions Science & Technology, 1999, 29(2):97-106.
- [5] Hansen E H, Løset S. Modelling floating offshore units moored in broken ice: Comparing simulations with ice tank tests [J]. Cold Regions Science & Technology, 1999, 29(2):107-119.
- [6] Hopkins M A, Shen H H. Simulation of pancake-ice dynamics in a wave field [J]. Annals of Glaciology, 2001, 33(1):355-360.
- [7] Zhan D, Agar D, He M, et al. Numerical Simulation of Ship Maneuvering in Pack Ice[C]// ASME 2010, International Conference on Ocean, Offshore and Arctic Engineering. 2010:855-862.
- [8] Michael Lau, Lawrence K, LeoRothenburg. Discrete element analysis of ice loads on ships and structures[J]. Ships & Offshore Structures, 2011, 6(3):211-221.
- [9] Shunying JI, Zilin LI, Chunhua LI, et al. Discrete element modeling of ice loads on ship hulls in broken ice fields [J]. Acta Oceanologica Sinica, 2013, 32(11):50-58.
- [10] LI Baohui, LI Hai, LIU Yu, et al. A modified discrete element model for sea ice dynamics[J]. Acta Oceanologica Sinica, 2014(1).

- [11] Yulmetov R, Lubbad R, Løset S. Planar multi-body model of iceberg free drift and towing in broken ice [J]. *Cold Regions Science & Technology*, 2016, 121:154-166.
- [12] Yulmetov R, Løset S. Validation of a numerical model for iceberg towing in broken ice [J]. *Cold Regions Science & Technology*, 2017, 138:36-45.
- [13] Gagnon R E. Results of numerical simulations of growler impact tests[J]. *Cold Regions Science & Technology*, 2007, 49(3):206-214.
- [14] Tsarau A, Lubbad R, Løset S. A numerical model for simulation of the hydrodynamic interactions between a marine floater and fragmented sea ice[J]. *Cold Regions Science & Technology*, 2014, 103:1-14.
- [15] Gilabert, F. A., J. -N. Roux, and A. Castellanos. "Computer simulation of model cohesive powders: Influence of assembling procedure." *Phys. Rev. E* 75 (2007): 011303.
- Hertz, H. "On the contact of elastic solids." *J. reine und angewandte Mathematik* 92 (1882): 156-171.
- [16] Mindlin, R. D. "Compliance of elastic bodies in contact." *Journal of Applied Mechanics* 16(1949): 259-268.
- [17] Mindlin, R. D., and H. Deresiewicz. "Elastic spheres in contact under varying oblique forces." *ASME*, September 1953: 327-344.
- [18] Løset S, Ø. Kanestrøm, Pytte T. Model tests of a submerged turret loading concept in level ice, broken ice and pressure ridges[J]. *Cold Regions Science & Technology*, 1998, 27(1):57-73.